A New Hand Measurement Method to Simplify Calibration in CyberGlove-BasedVirtual Rehabilitation

Jilin Zhou, François Malric, Shervin Shirmohammadi

Distributed Collaborative Virtual Environments Research (DISCOVER) Lab

School of Information Technology and Engineering (SITE), University of Ottawa, Canada

jzhou/fmalric/shervin@discover.uottawa.ca

Abstract— **We have previously developed a prototype virtual reality enhanced rehabilitation system using the CyberForce system to assist patients who have suffered from upper extremity stroke to practice some daily-life exercises. However, full calibration of the system for each patient is currently not only tedious and time-consuming, but also impractical in the case of severely disabled hands. In this paper, we propose a practical and easy-to-perform hand measurement method to calibrate the CyberGlove using artificial neural networks. The neural networks are trained with the hand segment sizes as input and the manually collected calibrated data as output. The only external device needed is a 2-D digital camera to take the picture of the subject's hand against a chessboard for the hand segment sizes measurement. Subjective evaluation results for various common hand postures show the effectiveness of the proposed method.**

Keywords- Virtual Rehabilitation, CyberGlove Calibration, Human Hand Measurement

I. INTRODUCTION

With recent advances in Human Computer Interfaces and Virtual Reality (VR) technologies, VR-enhanced stroke rehabilitation applications have been actively explored recently [1] [2]. These VR applications offer the potential to create systematic human testing, training and treatment environments which allow precise control of complex dynamic 3-dimensional (3-D) stimulus presentations, behavioral tracking, performance measurement, data recording and analysis [3] [4] [5]. At the Discover Lab, we have developed a prototype VR rehabilitation system to assist patients who have suffered from a stroke with upper extremity weaknesses [6] [7]. The physical setup of the prototype adopts the integrated CyberForce systems from CyberGlove Systems as shown in Fig. 1. The input measurements of the whole system include three parts: the whole hand translational position using the CyberForce subsystem, the rotation of the forearm using a 3-D magnetic tracker, and the hand gesture using a CyberGlove. One limitation of the system is that the motions of the elbow, the upper arm, and the shoulder are not measured which are in fact important to be monitored for upper extremity stroke rehabilitation. However, in the future, result of other on-going research about these limitations can be integrated into our system for the capture of the arm movements. For example, Hingtgen et al. present an upper extremity kinematic model which is able to accurately quantify upper extremity arm motion using a Vicon motion analysis system [8]. In [9], Zhou et al. proposed a data fusion-based tracking algorithm to estimate the upper limb movements using two wearable inertial sensors placed around the wrist and the elbow joints. To eliminate the problem of physically attaching sensors on the subjects' arm, Mihailidis et al studied the use of computer vision-based system in tracking of human motion in an intelligent environment [10]. However, presently it is still very challenging to track fine motor movements such as hand or arm movements with these methods, and more research is still needed in this area.

Figure 1: CyberGlove system used in our haptic-enabled rehab system

The design requirements of our system were the results of several consultations with the Rehabilitation Centre of the Ottawa General Hospital. The prototype allows the patients to practice some daily-life exercises, such as moving common objects on the shelf, pouring tea into a cup, eating soup from a bowl, and tracing a maze without touching the walls. The initial implementation was also placed under the analysis of a group of five Occupational Therapists (OTs) that provided thorough feedback and further amendments to the system [6]. One of the main feedbacks from the OTs is that the calibration of the whole system is very tedious and time-consuming, particularly for the CyberGlove. CyberGlove is a kind of hand input device to measure human hand postures, so that the user can intuitively interact with the synthetic objects in a virtual environment in a natural way [11]. The glove used for this

study has a total of 22 sensors placed at critical points. Due to variations of the human hand size, the relative positions of the sensors to their correspondent critical points of the hand are different across the users. Calibration is therefore required. With the factory pre-installed calibration method, it takes takes about 5~10 minutes to get a decent calibration for a healthy person. This will be even more problematic in the case of rehab patients who have severe disability, to the extent that their hand's motor functions are not physically suitable for use in the normal calibration process.

Based on its applications, the existing calibration methods for CyberGlove fall into two categories. The first category focuses on the determination of the real joint angles of the hand with high accuracy [12] [13] [14], while the second category aims at achieving high visual fidelity of hand postures inside the virtual environments [15] [16] [17]. Accordingly, their respective evaluation methods are also different. For the first category, the performances are evaluated in terms of the absolute differences between the real values and their interpreted values inside the application. For the second category, the performances are evaluated by visually comparing the real world hand postures and their corresponding virtual representations. During calibration, the subjects are usually asked to pose different postures with their hand and move for an amount of time, or against some physical constraints. Therefore, for rehabilitation systems, simplifying the calibration process is not only a desirable feature for all patients, but also a necessary feature for some specific patients with more severe hand disability, without which the rehab itself cannot be performed.

In this paper we propose a practical calibration technique that is faster and simpler than existing methods, and can be more easily used by rehab patients even with severe upper extremity disability. Through the experiments, we found there are direct relationships between the human hand's segment size and the correspondent sensor's readings. In [18], we exploited this relationship for the sensors on the index, middle, ring, and pinky fingers and proposed a method using Artificial Neural Networks (ANNs) for the CyberGlove calibration. In fact, ANNs have been successfully applied for the calibrations of many systems in many different engineering fields for its usage simplicity and effectiveness in learning complex underlying input/output patterns [19] [20] [21] [22]. In this paper, we have retrained the neural networks with different input/output combinations that were missing in [18], such as hand width, and also extended the method to measure the thumb and abduction related sensors, which is physically different and more difficult from the other fingers. In addition, we've performed subjective evaluations with five common hand postures which show the effectiveness of the proposed method.

The rest of the paper is organized as follows. Section II discusses the background and the related work. Section III details the procedures of our proposed method: measuring hand segment size, collecting calibration data, and training neural networks. Section IV presents the experimental evaluation and results of the proposed method. Finally, Section V concludes the paper and outlines the future work.
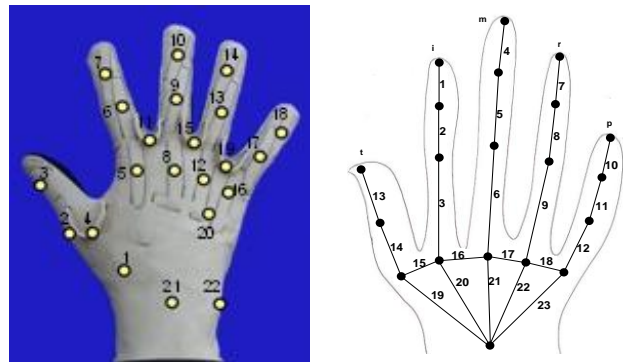

Figure 2: (a) Instrumented CyberGlove and sensor indexing, and (b) hand segments indexing used in the research.

II. BACKGROUND AND RELATED WORK

There are a total of 22 sensors on the CyberGlove, which are placed at critical points for the measuring of finger flexing, abduction, thumb roll, palm arch, wrist yaw, and pitch as shown in Fig. 2a. The sensors are light, thin strips sewn into the glove fabric. The output of each sensor is an 8-bit unsigned integer in the range of 0-255. Since all joint movements are less than 180 degree, 8-bit output provides a sub-degree resolution. Given a sensor's raw data reading x, its corresponding joint angle is calculated as

$$\theta = g(r - x), \qquad (1)$$

where g and r denote the sensor gain and offset respectively. Intuitively, the calibration process is to find this gain and offset for each sensor so that the user's hand gesture in the real world can be faithfully reproduced in the virtual environment. For example, when the thumb tip and the index tip are touched together in the real world, there should be no obvious gap between the correspondent configurations in the virtual world. Since hand sizes for different users are different, the relative positions of sensors to the correspondent critical points of the hand are different across the users. Calibration is therefore required to adapt to each user's hand size and to convert sensor output voltages to the joint angles. Even though most of the sensors are carefully decoupled by design, the number of sensors in total and their combined effects on the hand kinematics make the calibration not an easy task. For example, the readings from abduction sensors are affected by their adjacent meta-carpo-phalangeal (MCP) joints' flexion movements.

In [12], Griffin et al. present a calibration scheme to support dexterous tele-manipulation. The opening/closing movement of the end gripper on the robot manipulator is controlled by the distance between the thumb tip and the index finger tip. With their method, the user is first asked to place his/her thumb and index fingertips together and maintain a rolling contact while moving the fingers for 40 seconds. The readings from all of the related sensors during this period are recorded. After that, the separation distances between the two fingertips of a nominal hand kinematic model using the recorded data are calculated. Taking these separation distances as the errors to minimize, least squares method is then applied to tune all the related sensors' gain and offset to achieve an error-minimizing model

for each user. Menon et al. extended this method to all five fingers for the applications of virtual reality simulation for astronaut training and telemedicine [13]. In [14], Fischer et al. propose a nonlinear learning calibration using a neural network technique for a dataglove to control a four-finger robotic hand. The neural network is trained to learn the mapping from the dataglove data to the fingertips' positions. To get the actual Cartesian positions of the fingertips for the training, each of the four fingers is marked with a colored pin and two extra cameras are used. From the grabbed image and the known operating parameters of the cameras, the fingertips' positions are then recovered. The method can achieve fingertip position errors of less than 1.8 mm. However, this method has a number of limitations. First, this calibration method needs time synchronization between the dataglove data and the visual data. Second, two calibrated color cameras are needed to recover the 3-D Cartesian fingertips positions from the images. Third, only the positions of the fingertips are calibrated.

In our VR-based rehabilitation applications, we are more interested in the global visual satisfaction of all the joints involved in the hand movements inside the virtual environment than only absolute fingertips positions. As such, the above methods do not apply to our VR Rehab system. For example, when a patient practices holding a cup and moving it on a shelf, the contacts between the hand and the cup cannot be simplified into the contacts between the fingertips and the cup. It is very possible that the fingertips positions are correct but the middle joints are not.

There are other approaches that measure more than just the fingertips, but they also have their limitations. In [15] Kahlesz et al. propose a method to account for the cross-coupling effects between the MCP joints' flex sensors and the in-between abduction angles. For each abduction sensor, an iso-surface is created based on its readings under three experimental trajectories: only the left flex sensor bended, both left and right flex sensors bended, and only the right flex sensor bended. The values of this surface are stored in a look-up table for fast evaluation of the abduction angle. This is in contrast to the previously discussed methods which aim at the absolute accuracy of the joint angles between the virtual and the real hand. In [16], B. Wang et al. assume the effects from the neighboring flex movements are linear. Equation (1) then becomes

$$\theta_{abd} = g_{abd}(r_{abd} - x_{abd}) + (k_l r_l + k_r r_r + b), \qquad (2)$$

where r_{abd} is the calibrating abduction sensor's reading, g_{abd} and x_{abd} are the gain and offset of the sensor, r_l and r_r are adjacent MCP flexion sensor readings, k_l, k_r, and b are the cross parameters for the neighboring flexion sensors. During calibration, the subject needs to move the neighboring MCP joints both independently and jointly. Least square method is then applied to get these cross parameters. Following the same strategy, the authors calibrate the thumb related sensors. At this time, the subject is asked to constrain his/her index and thumb tips on to a bottle cap to compute the cross parameters. Both [15] and [16] focus on the coupling effects among the sensors. However, as will be seen in this paper, for the Rehabilitation

postures, the coupling effects among the sensors do not play an important role.

In [23], Kahol et al. propose a human anatomy based Hidden Markov Model (HMM) to recognize everyday human movements. Instead of modeling the gestures as sequences of static poses, the author suggested that they can be modeled as events occurring in the segments and joints of the human body. The events in joints are detected as stabilization of the angles between adjacent segments at the joints while the events for segments are detected as local minima in the segmental force. These two human anatomy-based HMMs are coupled together using the body distance between the segments and the joints. This gives us the idea that the hand movements can also be modeled as the events occurring in the hand segments and joints. The relationship between the selected hand segments size and the correspondent sensors reading can be exploited for the calibration of the CyberGlove.

III. THE PROPOSED METHOD

In this paper, we calibrate the sensors on the CyberGlove using ANNs. There are three main reasons for choosing ANNs for the calibration of the CyberGlove. First, ANNs have been successfully applied for the calibrations of many systems in many different engineering fields. In [19], a neural network is used to learn the mapping between the actual distorted image points and the corresponding pinhole camera image points to reduce the nonlinear effects of an imaging system based on CCD cameras. In [21], an industrial prototype microwave six-port instrument has been calibrated using the ANN technique which is able to achieve high accuracy over a wide dynamic range. In [20], R. Anchini et al. propose a neural network based method for the reconstruction of 3-D coordinates of object using the 2-D coordinates in two images planes from a dual-camera measurement system. In [22], J. M. Dias Pereira et al. apply an ANN for minimizing temperature drift errors of conditioning circuits and the experimental results show a significant improvement in the measurement accuracy. Second, we have noticed that there are some direct and consistent relationships between the human hand's segment size and the correspondent sensor's readings through the experiment. ANN is a very powerful tool to find such underlying pattern or relationships, even in a large dimension system. Third, once the final neural networks are found for each sensor, the generation of calibration data for any new subject is simple and fast. As mentioned above, simplicity of the calibration is very important for those patients with upper extremity weaknesses.

In our proposed method, the only external hardware needed is just a regular 2-D digital camera. We take a picture of the subjects' hand against a chessboard. From these 2-D images, we extract the sizes of the subjects hand segment. These hand segments sizes are the inputs for the neural networks. The chessboard here is used as the reference for the normalization of hand segments' size, so the zoom of the camera or the rotations of the hand relative to the chessboard do not affect the testing results. For the training of ANN, the outputs are the manually collected calibration data for these subjects. Different neural networks were trained with these experimental data for the sensors on the CyberGlove. The selection of the final neural

networks for each sensor is based on the minimum mean square error between the training sets and the evaluation sets.

In this section, the proposed method is elaborated in three steps: Measuring hand segments sizes, collecting calibration data, and training of the neural networks.

A. *Measuring hand segments sizes*

In order to calibrate the CyberGlove output, the manually calibrated results have to be related to the actual subject's hand size. We decided to take a picture of the subject's hand and compute the size of the hand segments with Matlab's image registration tool. The procedure is as follows. Predefined and visually identifiable locations on the hand, corresponding to the centre of each joint, the tip of each finger and the center of the wrist flexion, are marked with a color dot (we used blue for easy identification). The subject then places his/her hand against a chessboard. For that, there is no strict requirement on the camera except that the full hand image and chessboard is captured. This is also quite suitable for rehab patients, as no physical movement or hand action is necessary to take the picture. In Matlab, we create a same size chessboard as a reference and use the image registration tool to find the linear transformation between the raw image and this reference image as shown in Fig. 3. The image pixel selection tool is then used to get the positions of all the marked dots on the hand. From these dot positions, we compute the length of the segments defined in Fig. 2b. The segment sizes are normalized by using their ratio with the diagonal of the aligned image frame. This ensures that the measurements are independent of the camera resolution.

We have collected 25 subjects' right hand data for the training and the evaluation of the neural networks (22 men and 3 women, aged 22-38). The average length and standard deviation for each segment is plotted in Fig. 4. For the same segments, our collected hand parameters are generally consistent with the hand anthropometric data from Buchholz et al. in terms of the ratio of the segment to the hand length [24]. The small differences are due to the fact that our positioning of the wrist point is closer to the MCP joint. This general consistency supports our method of extracting the hand parameters from a 2-D hand image. Different from popular hand models, we do not consider the position of the carpo-meta-carpal (CMC) joint since it is not easy to be accurately located visually.
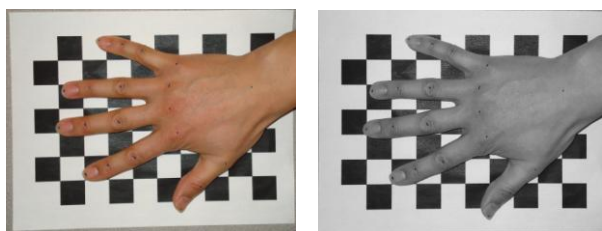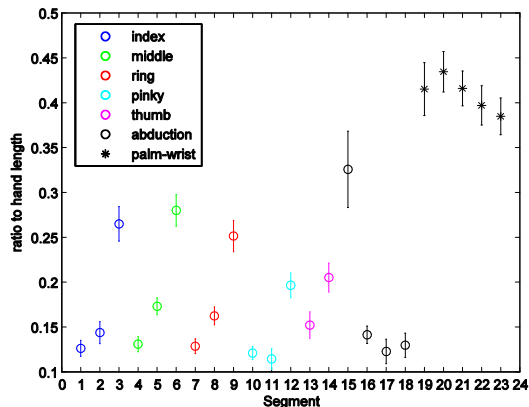

Figure 3: (a) Original image, (b) Aligned image

Figure 4: Statistics of hand segment sizes based on 25 subjects. References to the segments can be found in Fig. 2.

B. *Collecting calibration data*

Using the traditional technique that comes with standard CyberGlove system, calibration data for subjects were obtained by manually adjusting the gain and the offset of each sensor using the device control utility of the CyberGlove driver software. The device control utility provides a graphical hand model which renders the hand configuration in real time as the sensor's parameters are being adjusted. Fig. 5 illustrates the hand kinematic model used in our calibration. The kinematic model for the middle, the ring, and the pinky fingers are the same as that of the index finger. For sensors on each finger which measure the MCP, PIP, and DIP joints except the thumb, a subject is asked to keep the correspondent joint at zero degree first to get the offset for the sensor and then constraint at 90 degree to get the sensor gain according to (1). For some subjects who have difficulties in bending DP joints to 90 degrees, the constraints are set to 60 degrees. After the gain and the offset appear fine for these static poses, the subject then smoothly moves from one static pose to another static pose to make sure that there is no outlier situation during the hand movements. Using the same software, Lu and Huenerfauth designed a more detailed protocol for participants who are deaf and use American Sign Language [25]. Indeed, any calibration methods proposed by other researchers can be used here to collect the calibration data for the training of the neural networks.

Using this "standard" method, each calibration takes around 5 to 10 minutes for a healthy person. This tedious calibration process is mainly caused by the coupling effects of the sensor gain and its offset for the final joint angle as described in (1) and it tires the subject quickly. To minimize the subject bias, we calibrate each subject 3 times and all the calibrations start with a randomly generated calibration data. Calibration does not stop until both the operator and the subject agree that the calibration is satisfactory. The calibration for the thumb usually takes a longer time compared with that of the other ones. The main difficulty with the thumb calibration is that its movement simultaneously affects both the thumb roll and the thumb-index sensors. Even with bigger efforts, the subjects are generally more satisfied with the

calibration results of the index, the middle, and the ring fingers.
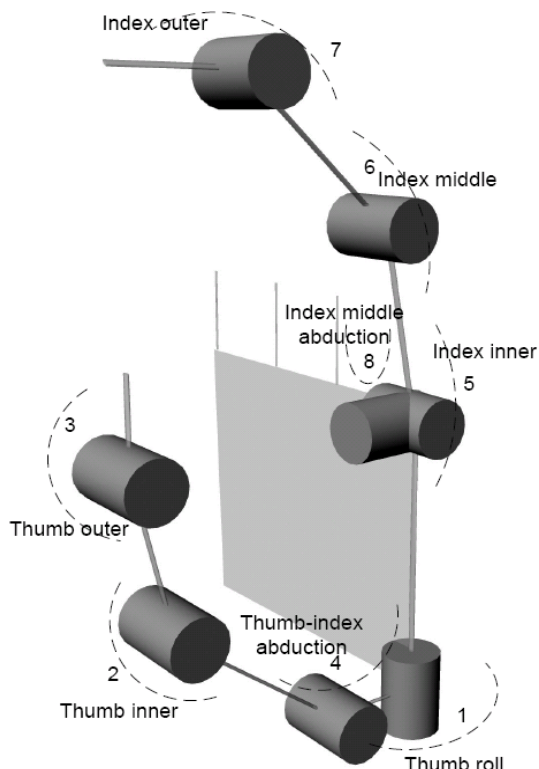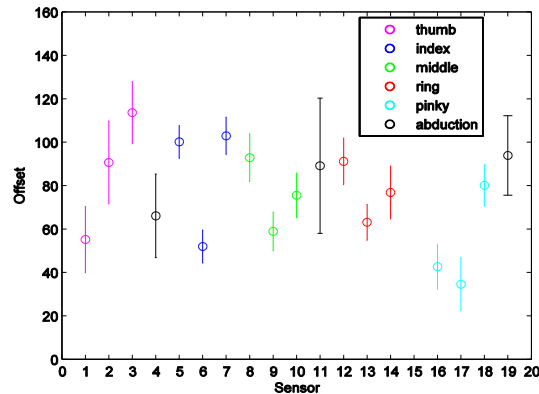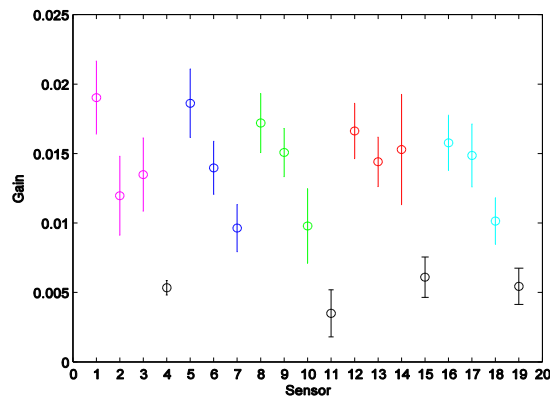

Figure 5: Hand kinematic model for calibration adapted from [25]. Refers to Fig. 2a for sensor indexing

(a)

(b)

Figure 6: Statistics of sensor values based on 28 subjects' calibration data: (a) offset, and (b) gain

Altogether, 75 sets of calibration data were collected for the training of the neural network. The mean and the standard deviation of the calibration data for all 19 sensors are plotted in Fig. 6a and Fig. 6b. Three sensors will not be covered in this paper: Sensor 20 which measures how much the pinky rotates across the palm toward the thumb, and Sensors 21 and 22 at the wrist which measure pitch and yaw of the palm relative to the wrist. Readings from Sensor 20 are not consistent while Sensor 21 and 22 are not considered because their relative positions to the hand vary every time the user puts the glove on.

It is interesting to see that Sensor 11 for middle-index abduction has the largest standard deviation for the sensor offset. At the same time, it has the smallest mean for the sensor gain. Considering the coupling effects between the sensor gain and offset for the final joint angle as shown in (1), we cannot conclude that Sensor 11 has the largest variation among all the sensors across all the subjects. In fact, all 4 abduction sensors (Sensor 4, 11, 15, and 19) have a relatively large variation for the offset but a small mean for the gain. This is due to the fact that these abduction sensors are bending at the rest position while other sensors are flat at the rest position as illustrated in Fig. 2a. In this regard, the offset and gain of the sensor does vary for different hand sizes. It is exactly this relationship between the hand size and the correspondent calibration results we are exploiting in this paper.

TABLE I.   INPUT-OUTPUT RELATIONSHIP FOR NN TRAINING

Input Hand Segments(Fig. 2b)	Output Sensor Number (Fig. 2a)	
1,2,3,24	Index°	5, 6, 7
4,5,6,24	Middle°	8,9,10
7,8,9,24	Ring°	12,13,14
10,11,12,24	Pinky°	16,17,18
13,14,19,24	Thumb°	1,2,3
19, 20,24	Thumb-index*	4
20, 21,24	Middle-index*	11
21, 22,24	Ring-middle*	15
22, 23,24	Pinky-ring*	19

°3 sensors on each finger, *abduction sensor, Segment 24 is the hand width calculated by adding segments 16, 17, and 18.

C. Training the Neural Networks

There are 3 sensors on each finger except the thumb for the measurements of the outer, the middle, and the inner joints respectively. For the thumb, there are also 3 sensors: the outer, the inner, and the roll sensors. Therefore, the networks used in the experiments have 3 inputs and 6 outputs for each finger

respectively. For each of the 4 abduction sensors, there are 3 hand segments contributing to the final joint angle. The relationship between the input and the output of the training neural networks are listed in Table I. Other machine learning methods could be employed to learn the relationships but here we use Artificial Neural Networks (ANN) given our previous positive experience with them [26].

There are a total of 75 sets of calibration data from 25 subjects (3 calibrations each) for the combined training and testing of the neural networks. The types of networks used in these experiments are regular feed-forward networks. The first obstacle faced was to properly choose the ANN architecture to solve our problem. We automate this selection task by using the workflow shown in Fig. 7. The architecture of the individual ANN is selected at random within a range of possible architectures. We allowed either 1 or 2 hidden layers with between 2 to 10 neurons each, and trained for 100 epochs, on 50-80% of the whole data (39 sets) – the rest were set aside for testing. The choice of these parameter ranges are believed to be sufficient for the type of relationship being modeled, as suggested by ANN guidelines [27] [28]. Levenberg-Marquardt learning algorithm is used for its good learning time in our testing. This type of ANN generation and training was performed 50 times, keeping the 5 best networks, the ones with the least mean square error on the validation data compared with the original calibration results. The final generated calibration data is the averaged results of these five best neural networks. It should be noted that the whole procedure of obtaining calibration data, generating the ANNs, training, and testing them will yield results specific to the system from which the data originated; they might not apply to other systems.
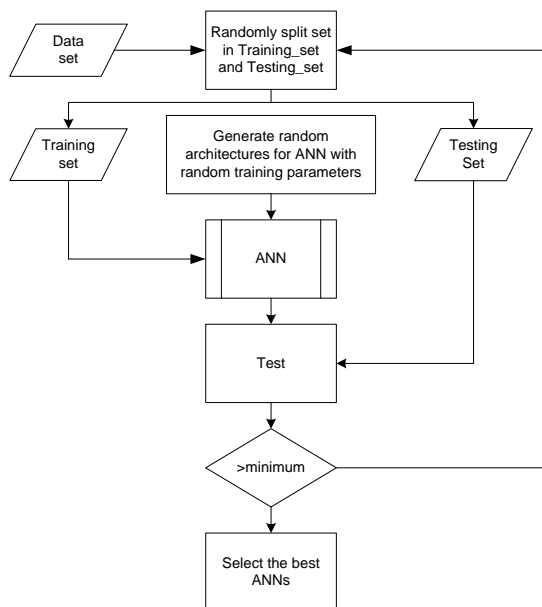

Figure 7: ANN architecture generation workflow

IV. RESULTS AND DISCUSSIONS

The mean and the standard deviation of the error between the final testing results (output of the ANNs for all subjects) and the original calibration data are plotted in Fig. 8a and Fig.

8b respectively. For the sensor's offset calibration, the average mean error for all 19 sensors is 0.4642. Among them, four abduction sensors have the largest error standard deviations. This conforms to the original collected calibration data where the abduction sensors also have the largest offset standard deviations as shown in Fig. 6. Three thumb sensors have relatively large error standard deviations compared with those on the other four fingers. For the analysis, we normalize the error standard deviation in terms of its ratio to the correspondent sensor's mean offset. The result is plotted in Fig. 9. In this regard, Sensor 1 (thumb roll) and Sensor 4 (thumb-index abduction) have the largest errors of 0.2586, and 0.2543 respectively. If we only consider the sensors on the index, the middle, the ring, and the pinky fingers, the average error ratio for the sensor offset is 0.0645. For the sensor's gain calibration, the average mean error for all 19 sensors is 0.0001. Three thumb sensors have the largest standard deviation errors. After the normalization, the ratio of error standard deviation to the correspondent sensor's mean gain is plotted in Fig. 10. Sensor 11 (middle-index abduction) has the largest error of 0.3045. On the other hand, referring to Fig. 6b, the mean of Sensor 11's gain is actually the smallest, so its effects on the final joint angles are not so formidable. If we only consider the sensors on the index, the middle, the ring, and the pinky fingers, the average error ratio for the sensor gain is 0.0731.

If we analyze the offset and the gain errors between the testing results and the original calibrated data together, they are quite uniform for all the sensors on the fingers excluding the thumb. For the thumb sensors, there are two main reasons for the large error variations. First, we did not take into account the position of the CMC joint in our hand parameter extraction while it is directly related to the thumb roll and the thumb-index abduction sensor. Instead, we expected the neural networks to learn the relationship through the sizes of Segment 19, 20, and 24 (Referring to Fig. 2b). However, since we were not strict on the position of the thumb when the hand pictures were taken, the variances of Segment 19 do not reflect the real situation faithfully. Second, as aforementioned, the collected calibration data for thumb roll and thumb-index abduction sensors are not as good as other sensors. Since both the input and the output for the training of the neural networks for the thumb sensors suffer from the reliability, it is not surprising to have large error variations among the related sensors.
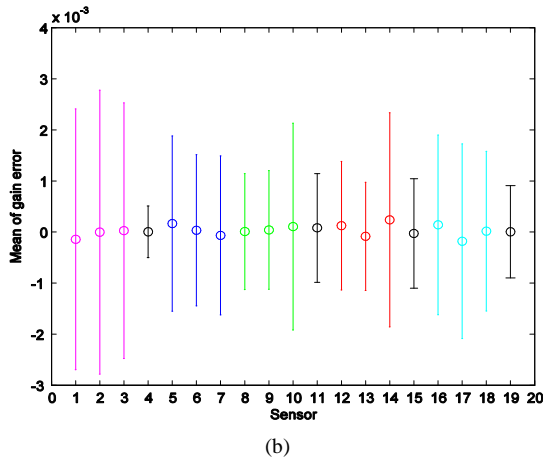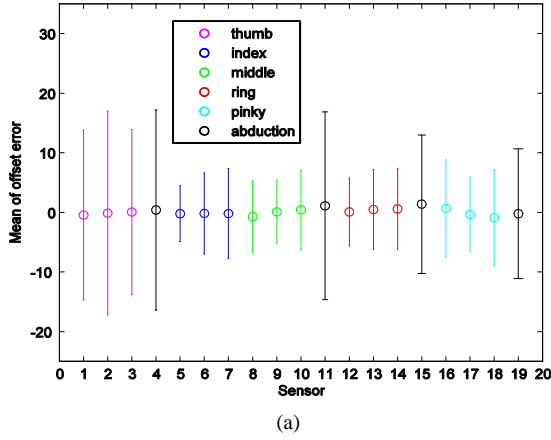
(a)

(b)

Figure 8: Statistics of test results and the original calibration data: (a) Offset error, and (b) Gain error
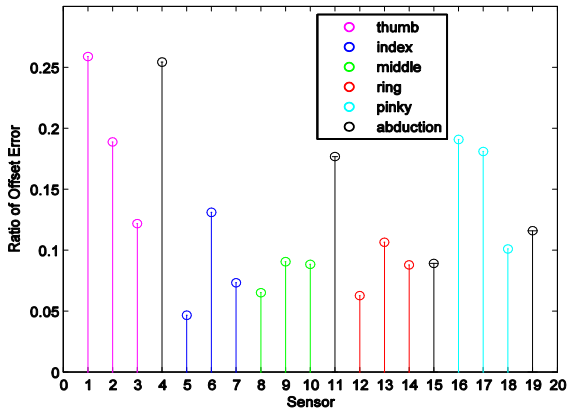

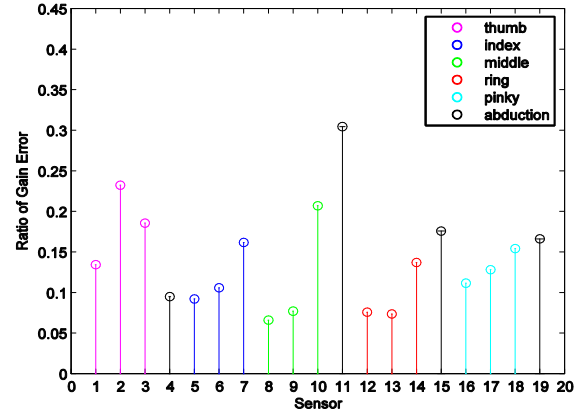Figure 9: Ratio of the offset error standard deviation to the corresponding sensor mean offset

Figure 10: Ratio of the gain error standard deviation to the corresponding sensor mean gain

A. Subjective Evaluation

The overall performance of the proposed method is tested both on subjects whose data were used and on subjects whose data were not used in the training process. From their hand parameters extracted from the pictures, the corresponding calibration data were generated using the trained neural networks. Altogether, 15 subjects were involved in the testing. Five of them were used in the training set. The subjects gave a score for sensors on each finger with a value from 1 up to 5 inclusive, with 1 being the most negative answer, 3 being acceptable and 5 being the most positive one. Five gestures used in the manually collection of the calibration data were evaluated. The average results are listed in Table II.

Table II: Subjective Evaluation Results

Posture	T	I	M	R	P	A	TA	Ave
	4.70	4.38	4.5	4.54	4.25	4.42	4.62	4.48
	4.62	4.08	3.66	4.21	4.20	4.25	4.54	4.23
	4.41	4.0	3.79	4.04	4.29	4.5	4.41	4.20
	4.0	4.38	3.95	4.45	4.25	3.95	4.16	4.16
	4.29	3.87	3.91	3.92	3.83	3.79	4.33	3.99

T: thumb; I: Index; M: middle; R: ring; P: pinky;
A: abduction sensors; TA: thumb abduction sensors; Ave: Average

In general, the results for all five postures are positive which proves the relationship between the measured hand segment size and the calibration parameters. It is reasonable that the first posture gets the highest average score since all the sensors are in the zero state. Another noticeable fact is that the results for the subjects in the training sets are better that those not in the training sets. This suggests that more subjects are needed for more distributed training sets. Posture 5 is mainly used for the testing of the 5 abductions sensors. Interestingly, this posture also affects the reading for the MCP joints since these

flexion sensors are bended in another direction. There are occasionally not acceptable results for some joints.

B. Comparison with Existing Methods

Compared with the standard calibration technique for CyberGlove, which takes about 5 to 10 minutes, our proposed method is very simple to use and the experimental results are also promising. The only external device needed is a 2-D digital camera to take the subject's hand picture. The whole process can be easily automated and lasts no more than a minute. This simplicity and quickness is extremely important to the CyberGlove based haptic rehabilitation system where the patient may have difficulties to finish the calibration if the procedure takes too long or complex.

No direct comparison can be made between our work and that in [12] and [13] since the collection of the calibration data for the training of the neural network is different. In those two papers, the authors focused on the coupling effects among the sensors while those coupling effects are not considered in the factory manual calibration software used for our collection of the training data. However, for the five tested postures, the coupling effects among the sensors do not play important roles.

Finally, it should be noted that the proposed method is not meant to replace current techniques. Instead, it is a new approach where any existing calibration techniques, including [15] and [16], can be used as input to the training of the neural networks. We do believe the inclusion of these coupling effects for the collection of the training data will further improve the experimental results and expand the application of the proposed method to more diversified hand postures.

V. FUTURE WORK AND CONCLUSION

Currently calibration of the CyberGlove is time-consuming and depends on the experience of the operator on the calibration routine. A good calibration may take about 5~10 minutes for a single user due to the large number of DOFs of the hand and the number of sensors on the data glove. This tedious calibration process should be especially avoided in VR-based rehabilitation applications where the patients may not be able to complete the physical movements required for the calibration. In this paper, we proposed a practical calibration method for the CyberGlove using neural networks. The inputs to the neural networks are the sizes of the hand segments which can influence the corresponding sensors of the CyberGlove, and the outputs are the offset and the gain for each sensor. In this way, only a 2-D hand picture is required for the generation of the required calibration data. Another advantage of the method is that it is not a replacement of the calibration techniques proposed by other researchers. Any other calibration methods can be used for the collection of data sets for the training of the neural networks.

In our current implementation, we have manually collected 25 subjects' calibration data for the training of the neural networks. Different neural networks with random parameters have been generated with random sets of the training data and the testing data. The best 5 neural networks for each sensor which had the least mean square errors between the training set and the testing set were saved. We've tested the resulting

neural networks for 15 subjects using 5 common hand postures. The subjective results are very positive. The error analysis shows that the variations for the sensors on the index, the middle, the ring, and the pinky finger are quite uniform while the thumb and abduction related sensors have larger variations. However, the performance for the subjects in the training set is slightly better than those not in the training set. This suggests that more distributive training sets are needed.

As we have noticed during the calibration process, the thumb-index abduction sensor and the thumb roll sensor are the most time-consuming due to their coupling effects. We have also noticed that the thickness of the human hand varies a lot. We also did not consider the cross-coupling factors such as adjacent MCP joints' flexion movement on the abduction sensors. We believe that the inclusion of these factors will further improve the results and expand the application of the proposed method for more diversified hand postures. Finally, we will automate the whole calibration procedure and integrate it into our rehabilitation system.

REFERENCES

[1] A. Henderson, N. Korner-Bitensky, and N. Levin, "Virtual reality in strock rehabilitation: a systematic review of its effectiveness for upper limb motor recovery", *Topics in Strock Rehabilitation*, vol. 14, no. 2, pp. 52-61, Mar-Apr. 2007.

[2] J. Crosbie, S. Lennon, M. McNeill, and S. McDonough, "Virtual reality in the rehabilitation of the upper limb after stroke: the user's perspective", *Cyberpsychology & Behavior*, vol. 9, no. 2, pp. 137-141, Apr. 2006.

[3] M. McLaughlin, A. Rizzo, Y. Jung, W. Peng, S. Yeh, W. Zhu, and the USC/UT Consortium for Interdisciplinary Research, "Haptics-enhanced virtual environments for stroke rehabilitation", in *Proc. of the IPSI*, Cambridge, MA. 2005.

[4] D. Jack, R. Boian, A. S. Merians, M. Tremanine, G. C. Burdea, S. V. Adamovich, M. Recce, and H. Poizner, "Virtual reality-enhanced stroke rehabilitation", *IEEE Transaction on Neural Systems and Rehabilitation Engineering*, vol. 9, no. 3, Sep. 2001, pp. 308-318.

[5] E. Todorov, H. Shadmehr, and E. Bizzi, "Augmented feedback presented in a virtual environment acclerates learning of a difficult motor task," *Journal of Motor Behavior*, vol. 20, no. 2, pp. 147-158, 1997.

[6] R. Kayyali, A. Alamri, M. Eid, R. Iglesias, S. Shirmohammadi, A. El Saddik, and E. Lemaire, "Occupational therapists' evaluation of haptic motor rehabilitation", in *Proc. of IEEE Conference of Engineering in Medicine and Biology Society*, Lyon, France, Aug. 23-26 2007, pp. 4763-4766.

[7] A. Alamri, M. Eid, R. Iglesias, S. Shirmohammadi, A. El Saddik, "Haptic virtual rehabilitation exercises for post-stroke diagnosis", *IEEE Transactions On Instrumentation and Measuremen*Vol. 57, Issue 9, Sept. 2008, pp. 1876 – 1884.

[8] B. Hingtgen, J. McGuire, M. Wang, and G. Harris, "An upper extremity kinematic model for evaluation of hemiparetic stroke," *Journal of Biomechanics*, vol. 39, no. 4, pp. 681-688, 2006.

[9] H. Zhou, H. Hu, J. Hammerton, and N. Harris, "Applications of wearable inertial sensors in estimation of upper limb movements," *Biomedical Signal Processing and Control*, vol. 1, no. 1, pp. 22-32, Jan. 2006.

[10] A. Mihailidis, B. Carmichael, and J. Boger, "The use of computer vision in an intelligent environment to support aging-in-place, safety, and independence in the home," *IEEE Transactions on Information Technology in Biomedicine*, vol. 8, no. 3, pp. 238-247, Sep. 2004.

[11] G. D. Kessler, L. F. Hodges, and N. Walker, "Evaluation of the CyberGlove as a whole-hand input device", *ACM Transactions on Computer-Human Interaction*, vol. 2, no. 4, pp. 263-283, Dec. 1995.

[12] W. B. Griffin, R. P. Findley, M. L. Turner, and M. R. Cutkosky, "Calibration and mapping of a human hand for dexterous telemanipulation," in *Proc. of the ASME IMECE Dynamics Systems and Controls Division*, vol. 69, 2000, pp. 1145-1152.

[13] A. S. Menon, B. Barnes, R. Mills, C. D. Bruyns, E. Twombly, J. Smith, K. Montgomery, and R. Boyle, "Using registration, calibration, and robotics to build a more accurate virtual reality simulation for astronaut training and telemedicine", in *Proc. Of WSCG 2003,* Czech Republic, Feb. 3-7, 2003.

[14] M. Fisher, P. Smagt, and G. Hirzinger, "Learning techniques in a dataglove based telemanipulation system for DLR hand", in *Proc. Of the 1998 IEEE International Conference on Robotics & Automation*, Leuven, Belgium, May 1998, pp. 1603-1608.

[15] F. Kahlesz, G. Zachmann, and R. Klein, "Visual-fidelity dataglove calibration", in *Proc. of the Computer Graphics International (CGI'04)*, 2004, pp. 403-410.

[16] B. Wang, and S. Dai, "Dataglove calibration with constructed grasping gesture database", *IEEE International Conference on Virtual Environment, Human-Computer Interfaces and Measurements Systems (VECIMS ,09)*, Hong Kong, China, May 11-13, 2009, pp. 6-11.

[17] P. Liu and M. Huenerfauth, "Accessible motion-capture glove calibration protocol for recording sign language data from deaf subjects", *in Proc. of the 11th International ACM SIGACCESS Conference on Computers and Accessibility (ASSETS 2009)*, Pittsburgh, PA, USA, Oct. 26-28, 2009.

[18] J. Zhou, F. Malric, and S. Shirmohammadi, "Practical calibration for upper extremety patients in haptic rehabilitation", in *Proc. of IEEE International Workshop on Medical Measurements and Applications*, Cetraro, Italy, May 29-30, 2009, pp. 73-78.

[19] D. Choi, S. Oh, H. Chang, and K. Kim, "Non-linear camera calibration using neural networks", Neural, Parallel & Scientific Computations, vol. 2, no. 1, pp. 29-42, Mar. 1994.

[20] R. Anchini, C. Liguori, V. Paciello, and A. Paolillo, "A comparison between stereo-vision techniques for the reconstruction of 3-D coordinates of objects", *IEEE Transactions on Instrumentation and Measurement*, vol. 55, no. 5, pp. 1459-1466, Oct. 2006.

[21] Y. Liu, "Calibrating an industrial microwave six-port instrument using the artificial neural network technique", *IEEE Transactions on Instrumentation and Measurement*, vol. 45, no. 2, pp. 651-656, Apr. 1996.M. L.

[22] J. M. Dias Pereira, O. Postolache, P. M. B. Silva Girão, and M. Cretu, "Minimizing temprature drift errors of conditioning circuits using artificial neural networks", *IEEE Transactions on Instrumentation and Measurement*, vol. 49, no. 5, pp. 1122-1127, Oct. 2000.

[23] K. Kahol, P. Tripathi, and S. Panchanathan, "Recognizing everyday human movements through human anatomy based coupled hidden markov model", *International Journal on Systemics, Cybernetics and Informatics*, Pentagram Publications, India, 2005.

[24] B. Buchholz, T. J. Armstrong, and S. A. Goldstein, "Anthropometric data for describing the kinematics of the human hand", *Ergonomics*, vol. 35, no. 3, pp. 261-273, 1992.

[25] M. L. Turner, "Programming Dexterous Manipulation By Demonstration", *Ph.D thesis*, Stanford University, Jun. 2001.

[26] F. Malric, A. El Saddik, N.D. Georganas, "Artificial Neural Networks for Real-Time Optical Hand Posture Recognition Using a Color-Coded Glove", *in Proc. IEEE Conference on Computational Intelligence for Measurement Systems and Applications (CIMSA08)*, Istanbul, Turkey, Jul. 2008, pp. 105-110.

[27] B. G. Lipták, *Instrument Engineers' Handbook: Process control and optimization*, 4th Edition, CRC Press, 2006.

[28] H. Demuth, and M. Beale, *NeuralNetwork Toolbox User's Guide*, Version 4, The Matworks Inc., 2004.